Graphene Oxide. Origin of Acidity, Its Instability in Water, and a New Dynamic Structural Model

Ayrat M. Dimiev,[†] Lawrence B. Alemany,[†,¶,⊥] and James M. Tour[†,‡,§,⊥,*]

[†]Departments of Chemistry, [‡]Mechanical Engineering and Materials Science, and [§]Computer Science, the [⊥]Smalley Institute for Nanoscale Science and Technology, and the [¶]Shared Equipment Authority, Rice University, MS-222, 6100 Main Street, Houston, Texas 77005, United States

ABSTRACT The existing structural models of graphene oxide (GO) contradict each other and cannot adequately explain the acidity of its aqueous solutions. Inadequate understanding of chemical structure can lead to a misinterpretation of observed experimental phenomena. Understanding the chemistry and structure of GO should enable new functionalization protocols while explaining GO's limitations due to its water instability. Here we propose an unconventional view of GO chemistry and develop the corresponding "dynamic structural model" (DSM). In contrast to previously proposed models, the DSM considers GO as a system, constantly changing its chemical structure due to interaction with water. Using potentiometric titration, ^{13}C NMR, FTIR, UV—vis, X-ray photoelectron microscopy, thermogravimetric analysis, and scanning electron microscopy we show that GO does not contain any significant quantity of preexisting acidic functional groups, but gradually generates them through interaction with water. The reaction with water results in C—C bond cleavage, formation of vinylogous carboxylic acids, and the generation of protons. An electrical double layer formed at the GO interface in aqueous solutions plays an important role in the observed GO chemistry. Prolonged exposure to water gradually degrades GO flakes converting them into humic acid-like structures. The proposed DSM provides an explanation for the acidity of GO aqueous solutions and accounts for most of the known spectroscopic and experimental data.

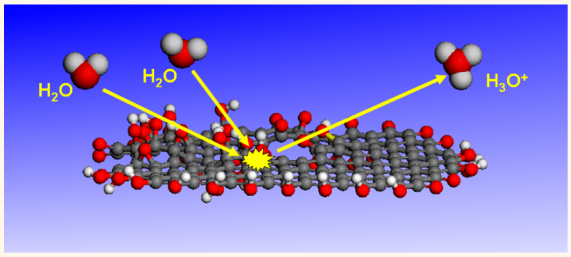

KEYWORDS: graphene oxide · acidity · dynamic structural model · graphene interaction with water

Graphene oxide (GO) is a single layer of carbon atoms from an original graphene lattice that has been oxidized to form C—O bonds.[1] The bulk form of GO, conventionally named graphite oxide, has attracted recurring interest from the chemist community since it was first synthesized by Brodie in 1855.[2] Historically several structural models of GO have been developed,[3−10] but none of them account for all of the known experimental data. Despite much research, the structure of GO remains elusive. A new interest in GO was sparked after the discovery of graphene; it was found that upon reduction GO can serve as the precursor for chemically converted graphene (CCG).[11−13] GO and its functionalized derivatives have also been successfully tested in numerous applications in optoelectronics, biodevices, drug delivery systems, and composites.[1] Upon dissolution in water with sonication, or even simple swirling, bulk graphite oxide spontaneously exfoliates to single layer GO sheets. From this perspective, bulk graphite oxide can be considered simply as an accumulation of GO flakes. In this work we will use the term "GO" to signify both single atomic layer sheets and their bulk form.

According to recent studies,[9,10] each GO layer is considered as a multifunctional network, containing several oxygen functionalities in addition to the carbon backbone. The Lerf—Klinowski (LK) model[9] concludes that GO consists of two different randomly distributed domains: (a) areas of pure graphene with sp^2-hybridized carbon atoms and (b) areas of oxidized and thus sp^3-hybridized carbon atoms. The oxidized GO domains contain epoxy and hydroxyl functional groups; carboxyl and hydroxyl groups terminate the flake edges. The Szabo—Dekany (SD) model,[10] which is in turn the further development of the earlier proposed Clauss[5] and Scholz[6] models, represents GO as a periodic ribbon-like

* Address correspondence to tour@rice.edu.

Received for review October 12, 2012 and accepted December 5, 2012.

Published online December 05, 2012
10.1021/nn3047378

© 2012 American Chemical Society

structure of aromatic and nonaromatic domains. The oxygen functionalities that are thought to be present are hydroxyls and four-membered ring ethers. The SD model suggests that ketones and quinones are formed where C−C bonds have been cleaved. The GO images recently obtained by high resolution transmission electron microscopy (HRTEM)[14] support the LK two-type-domain model. In addition to intact graphene domains and oxidized domains, as was predicted by LK, nm-sized holes were observed in GO flakes. Interestingly, even aberration-corrected HRTEM[14] did not shed further light on the GO chemical structure. Most of the recently published GO-related studies employ exclusively the LK model to interpret experimental data. The ideas suggesting C−C bond cleavage and the formation of ketones proposed in the SD model are underappreciated. This leads to confusion in understanding the nature of reactions involving GO.

GO has a variable stoichiometric ratio of the constituent elements that depends in part on the oxidation level. However, regardless of the preparation method used,[2,15,16] all the GO samples have the same set of functional groups. The GO composition and structure do not change significantly with addition of excess oxidizing agent after achieving some threshold oxidation degree.[10,17] Thus all of the solid state nuclear magnetic resonance (SSNMR),[7,9,10,17−19] Fourier transform infrared (FTIR) spectra,[7,10,17,19] and X-ray photoelectron spectroscopy (XPS)[10−13] spectra of the GO products prepared by several general methods are qualitatively similar, suggesting the same set of oxygen-containing functional groups.

One of the peculiar properties of GO is the high acidity of its aqueous solutions, which is difficult to harmonize with the current models. Aqueous GO solutions have a pH of ~3, and 100 g of GO contains 500 to 800 mmol[3,5] of acidic sites that can take part in cation exchange reactions. This is approximately 1 acidic site for every 6−10 carbon atoms. The cation exchange ability, along with the LK suggestion regarding the presence of carboxyl groups on the flake edges, led many researchers to think that carboxyl groups do exist in GO, and that they are the entities responsible for the acidic properties of GO. Along this line, suggested reactions between carboxyl moieties on GO and exogenous amines are affected by this interpretation from the LK model. Indeed, the classical representation for the cation exchange reaction involves conversion of carboxyls to carboxylates. It is unlikely, however, that the small number of carboxylic acid moieties situated on the edges of the GO flake, as proposed by the LK model, can account for such a high cation exchange capacity. Even defect (hole) edges cannot host so many carboxyls. Finally, a high content of carboxyls is not supported by NMR and XPS spectroscopy data.[8−13,17−19] To the best of our knowledge, no report has been published where the GO acidity was explained in accordance with existing spectroscopic data. At the same time, as will be shown below, acidity is the key factor in understanding the GO chemistry and structure.

Another interesting GO property is its ability to deoxygenate under strong alkaline conditions,[20] or to be "reduced",[21,22] when no reducing agent is present. The mechanism of this reaction is not clear, and this leads to misinterpretation of the observed phenomena.[21,22]

In our previous report[17] we demonstrated that the as-prepared GO, which was referred to as "pristine GO", upon exposure to water undergoes gradual transformations. This results in the extension of conjugated areas, causing color change. In this report we further develop the earlier proposed reaction mechanism and show that reaction with water is a key factor in understanding the acidity of GO. To arrive at this conclusion, a detailed study of the acidic properties of GO was performed; the structure of GO as a function of pH was investigated. As a result of these studies, a new structural GO model is proposed that is in accord with most of the known experimental facts. The model is termed the dynamic structural model (DSM). A proposed mechanism for the deoxygenation of GO in alkaline solutions and for degradation of GO in water is also presented.

RESULTS AND DISCUSSION

Concentration of Acidic Sites and Their pK_a Values. By considering GO as a weak acid one can calculate the concentration of acidic sites in solution and their pK_a values based on pH values measured at different solution concentrations. This approach assumes that the acidic groups behave as independent entities and that only one type of acidic group is present. This simplified model is not correct since the acidic groups are probably located on adjacent or conjugated carbon atoms, affecting their ionization. Furthermore, as detailed below, there are additional factors contributing to the acidity. Nevertheless, these experiments can give a rough estimate of the acidic properties of GO. To the best of our knowledge, such experiments and determinations, despite their simplicity, have never been reported. The measured pH values for the three aqueous solutions with GO content of 1.0, 0.5, and 0.25 mg/mL were 3.37, 3.54 and 3.72, respectively. The calculations reveal the concentration of acidic sites in the most dilute solution as 5.0×10^{-4} mol/L. Accounting for the GO content in solution, this yields one acidic site per 25 carbon atoms. The calculated pK_a values are in the range of 3.93−3.96, suggesting that GO is a stronger acid than commonly known carboxylic acids with a single functional group in a molecule.

To quantitatively assess GO acidic properties, a series of potentiometric titrations was performed. Traditionally the "Boehm titration protocol" is used to

determine the content of oxygen functionality in carbon-based materials.[23] It is based on the idea that oxygen functionalities have different acidities and can be neutralized by bases of different strengths. According to the protocol, the sample is equilibrated with base (aqueous NaOH, Na_2CO_3, or $NaHCO_3$) for 24 h, then the filtered solution is acidified with a known quantity of aqueous HCl, and finally back-titrated with aqueous NaOH. As shown below, this technique conceals crucial information regarding the chemistry of GO. Direct titration provides much more information about the nature of the sample. While direct GO titration was rarely used in the studies related to GO structure, to the best of our knowledge, potentiometric reverse titration has not been reported. It was found earlier that GO titration curves do not have distinguishable inflection points, which was interpreted to mean that the pK_a regions of the numerous acidic functional groups overlap.[24,25] This conclusion, however, contradicts all the structural studies[7−13,17−19] showing that GO samples contain a definite and limited set of functional groups. According to the ^{13}C SSNMR[7,9,10,17−19] data, there is only one type of functional group (a small peak at 167 ppm which can be assigned to carboxyl carbons) capable of protonating water, and thus function as an acid. Therefore, the suggestion that GO contains multiple acidic groups[24,25] is not correct. We propose another explanation for the lack of the inflection points on titration curves. As will be detailed below, GO does not contain any significant quantity of preexisting acidic functional groups, but gradually generates them *via* interaction with water. Several phenomena involving an electrical double layer at the GO interface might additionally contribute to the lack of inflection points.

It was noted earlier that the data related to the acidic properties of GO is inconsistent. Thus the number of functional groups taking part in cation exchange reactions was found to vary from 250 to 1400 mmol per 100 mg of sample.[3,5] In our studies it was found that the data obtained from different titration experiments using the same GO sample depended significantly on the titration procedures. The implication of these inconsistencies is that our understanding of the GO chemical structure is not complete, and chemical reactions occurring during the titration affect the results of the titration. In the course of titration with aqueous 0.100 M NaOH, GO solutions gradually darken, changing from light-brown to very dark-brown. The original light color does not return during or after the reverse titration with aqueous 0.100 M HCl. Therefore the changes produced by the titration are irreversible and cannot be viewed as simple carboxylic acid−carboxylate conversion of common organic acids.

Figure 1a shows typical data obtained for GO titrations. The two titration curves labeled I and II correspond to forward and reverse titration according to

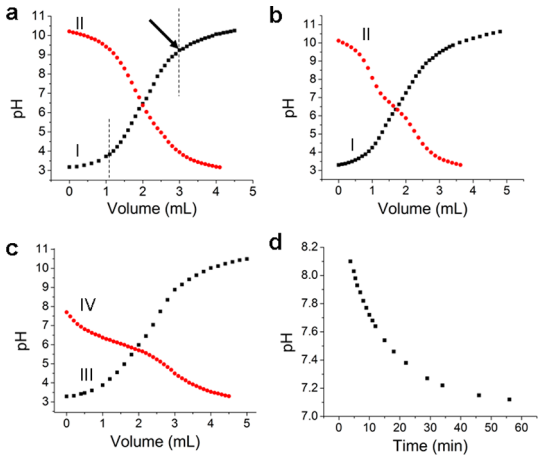

Figure 1. The GO titration curves. (a−c) Forward (black square) and reverse (red circle) titration curves. In the forward titration, the GO solution (1.0 mg/mL) was titrated with 0.100 M NaOH, and in the reverse titration, GO1, the conjugate base of GO was titrated with 0.100 M HCl. (a) The reverse titration was performed immediately after the forward titration. Dashed vertical lines on curve I arbitrarily separate the three titration zones discussed in the text. The black arrow indicates the accepted equivalence point. (b) Reverse titration was performed 6 h after the forward titration. (c) Titration curves (III) and (IV), which were performed after the titration (I) and (II) shown on panel a. The solution was heated at 60 °C for 15 h after the forward titration (III), and before performing the reverse titration (IV). (d) The change in pH of the GO solution with time after the addition of the 0.100 M NaOH solution. Zero time corresponds to the addition of NaOH. The increase in pH during the first 3 min 47 s after NaOH addition is not shown on the graph.

eqs 1 and 2:

$$GO + NaOH \rightarrow GO1 \quad (1)$$

$$GO1 + HCl \rightarrow GO2 \quad (2)$$

Curve I, reflecting the forward titration of the original GO sample, contains three distinguishable regions, separated by vertical dashed lines (Figure 1a): (1) short and slightly sloping with the first 1 mL of NaOH, (2) a long and continuously steep slope with the next 2 mL of NaOH, and (3) slightly sloping with the last 1 mL. In the first region, titration proceeds similar to titration of common acids: the pH changes immediately after the addition of a new portion of NaOH and will remain unchanged for hours if a new portion of NaOH is not added. In the second region the electrode's response slows and the pH increases very slowly; it takes 2−3 min to reach the final pH value. After reaching the highest value, the pH starts drifting downward and this drift continues if the new portion of NaOH is not added. This phenomenon of the downward drift of the pH is observed to be most significant in the 4.5−7.5 pH region. In this manual titration, the new portion of NaOH was added when the pH had reached the highest value and had not changed for ∼15 s, or after it started drifting downward and thus was lower than the maximum value by 0.01−0.02 pH points. Finally, in the

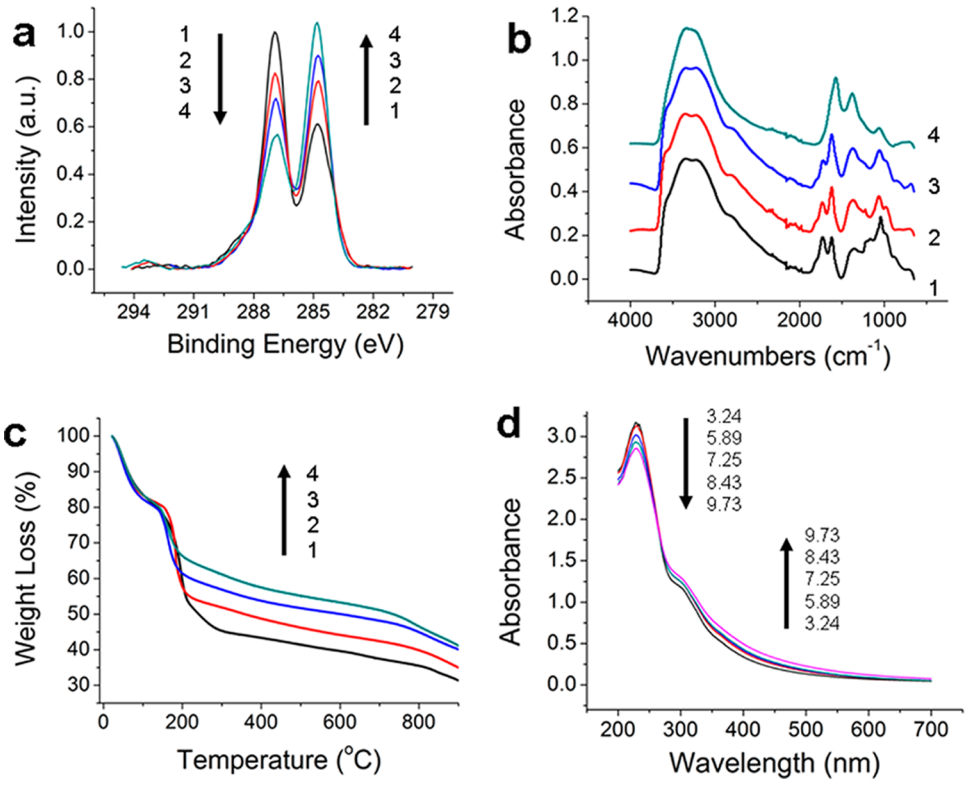

Figure 2. The characteristics of NaOH-GO samples recovered from solutions with different pH values. (a) C1s XPS, (b) FTIR, and (c) TGA data. The numbers 1, 2, 3, 4 on panels (a−c) refer to the solid GO samples recovered from solutions having pH values of 3.34, 4.50, 7.80, and 10.00, respectively. The corresponding line colors are black, red, blue, and green, respectively. (d) The UV−vis spectra of GO solutions with pH values indicated next to the arrows. Absorbance decreases in the UV region and increases in the visible region with increased pH.

third region, as the electrode again responds quickly, less pH downward drifting was noted.

From the shape of the titration curve I (Figure 1a), one could assume that the middle of the second region at pH ~6.5 is the equivalence point. It is not the case, however, because neutralization of the acidic sites continues during the entire second region (between dashed vertical lines) and even in the third region. In this work, to formally assess the content of acidic groups we considered the bending point of curve I at pH ~9.5 marked with a black arrow as the point where ~90% of the acidic sites are consumed. From numerous titration experiments with different GO samples, the calculated average value for the content of acidic sites was 1 per every 17 carbon atoms, while the highest value was $^1/_{12}$ and the lowest value was $^1/_{23}$. This result is higher than $^1/_{25}$ obtained from the experiment with GO solutions of different concentrations, described above. Thus, addition of the NaOH solution facilitates generation of additional protons when compared to dilution with pure water. At the same time the obtained titration data ($^1/_{17}$) is significantly lower than the cation exchange ability ($^1/_6$—$^1/_{10}$) reported in the literature.[3,5] The acidic sites, generating protons, are not likely to be ordinary carboxyl groups, as is commonly thought. The presence of any significant amount of carboxyls on the GO platform is difficult to envision based on simple structural considerations. Every carbon atom in the original graphene lattice is connected to three neighboring carbon atoms. Therefore two out of three C−C bonds need to be broken to form a carboxyl from the original carbon backbone. Note that roughly half of the carbon atoms belong to graphene-type domains and therefore cannot be part of a carboxyl group. The structure with one carboxyl per remaining 3−5 carbon atoms simply cannot exist.

Acid Generation Capacity. The curve (II) (Figure 1a) represents the reverse titration, where GO1, the conjugate base of GO, is titrated with 0.100 M HCl. Note that less HCl equivalence is required in the course of the reverse titration to reach the initial pH value, compared to the corresponding amount of NaOH used for the forward titration. This is evidence for solution acidification, triggered by the addition of the NaOH solution. If the reverse titration is not started immediately upon completion of the forward titration, the pH of the solution changed significantly between the titrations, which in turn changes the shape of the reverse titration curve. Figure 1b represents the titration experiment performed under the same conditions as the one in Figure 1a except that the reverse titration was started 6 h after completion of the forward titration. In this case, the reverse titration curve starts at

a slightly lower pH value due to additional solution acidification that occurred during those 6 h. There are two apparent inflection points on curve II (Figure 2b): at pH ~8.5 and at pH ~5.2. These are the points where the two different conjugate bases, formed during 6 h of standing, are titrated with HCl.

The pK_b values of the two conjugate bases, estimated based on the inflection points, are $pK_{b1} \approx 4.3$ and $pK_{b2} \approx 7.5$. From numerous titration experiments with different GO samples, we obtained values that range from 4.8 through 4.3 for pK_{b1}, and from 8.5 through 7.4 for pK_{b2}. These values are close to pK_b values of carbonate and bicarbonate, respectively, though not exactly the same. Considering the fact that the titration was done under nitrogen, and that no inflection points are present on curve I (Figure 1b), we conclude that CO_2 and/or another acidic entity was formed in the course of direct titration and upon 6 h standing. To exclude the possible contribution from CO_2 dissolved in water and/or in the titrant solution, we conducted control experiments by titrating a sample of pure water. No inflection points similar to those present on curve II (Figure 1b) were ever observed on the reverse titration curve. Note that in the experiment with 6 h standing (Figure 1b), even less HCl is required in the course of the reverse titration to reach the initial pH value, compared to the experiment shown in Figure 1a.

To assess GO's acid generation capacity, the GO2 solution after one cycle of forward−reverse titration was subjected to one additional titration cycle, according to eqs 3 and 4, where GO3 is GO2 that has been treated with NaOH, and GO4 is GO3 that has been treated with HCl (Figure 1c).

$$GO2 + NaOH \rightarrow GO3 \quad (3)$$

$$GO3 + HCl \rightarrow GO4 \quad (4)$$

More NaOH was added during titration III compared to titration I, and the solution after the forward titration was additionally kept 15 h at 60 °C to intensify the reaction between GO and NaOH. The pH of the solution dropped from 10.51 to 7.87 during that time (solution was kept under nitrogen), indicating significantly higher acidification compared to the experiment shown in Figure 1b. The two inflection points on the curve of reverse titration IV are again apparent (Figure 1c). Now the reverse titration curve starts in the middle of the first wave. The distance between the two inflection points is wider, suggesting that more conjugate base had been formed during 15 h at higher temperature. This experiment demonstrates that the acid generation capacity had not been exhausted during the first cycle of forward−reverse titration. Note that additional time and/or increased temperature are required for inflection points to appear on the reverse titration curves. Without these two factors, the reverse titration curve is featureless.

In a separate experiment we investigated the kinetics of an acid generation reaction. Figure 1d shows how the pH of a GO solution changes with time after a certain amount of NaOH is added to the original GO solution. The original sharp increase in pH caused by the NaOH addition is not shown on the graph. After reaching the maximum, the pH starts drifting downward and almost stabilizes within a few hours, but slow acidification continues for as long as a few days (not shown on the graph). The part of the curve shown (Figure 1d), is typical for kinetics of ordinary chemical reactions and suggests that hydrogen cations are generated in the course of a chemical process.

In our previous report[17] we showed that covalent sulfates are present in all the GO samples prepared by Hummers',[16] modified Hummers',[26,27] and Staudenmaier's[15] methods, but their presence was undetected or unreported by other researchers. To exclude the role of covalent sulfates as main contributors to observed GO acidity, we quantitatively determined their content in the GO samples (see SI for details). Experiments revealed that, though sulfates are present in significant quantities, their contribution to the integral GO acidity is less than one-third of the observed acidity (the total NaOH equivalent used for titration is 1 equiv). Note that GO samples prepared by Brodie's method do not contain covalent sulfates, but the GO is still acidic; apparently the acidity has another origin. The main factor contributing to GO acidity, as was mentioned above and will be detailed below, is the generation of protons during the reaction of GO with water. The amount of protons neutralized in the course of the GO titrations is significantly higher than the number of carboxyl groups that GO can possibly contain. In aqueous solutions, GO gradually generates hydrogen cations and this reaction is intensified by the addition of strong bases.

Characteristics of NaOH-Treated GO. To study the nature of this reaction, we investigated how the addition of NaOH to GO solution affects the nature of the GO oxygen functionalities. We will refer to GO samples collected from solutions of different pH levels with the addition of NaOH as NaOH-GO. Figure 2 represents XPS, FTIR, TGA, and UV−vis data for different NaOH-GO samples.

The C1s XPS spectrum (Figure 2a) of the original GO exhibits two major peaks, attributed to elemental carbon at 284.8 eV, and carbon of non-carboxyl carbonyls, alcohols, and epoxides at 286.6 eV. The latter is about twice the size of the former. The shoulder in the 288.0−289.5 eV region is associated with the carbon from the carboxyl groups. An increase in the pH of solution, from which GO was recovered, gradually decreases the 286.6 eV peak relative to the 284.8 eV peak, as evident from Figure 2a, suggesting significant deoxygenation. Note that the amount of carboxyls does not noticeably change relative to the combined amount of the other types of carbon.

The FTIR spectrum of GO samples (Figure 2b) is difficult to interpret due to the overlapping bands from numerous chemical bonds. The spectrum of the original GO displays the broad O−H stretch in the 3700−2400 cm^{-1} region. In the fingerprint region there are a series of overlapping bands with the most distinguishable one at 1039 cm^{-1}. In the literature, the relative intensities of the bands in this region and their interpretation differ from work to work and from sample to sample.[7,10,17,19,25] We think that due to the overlapping of many different bands, definitive assignment in this region is difficult. The most recognizable feature in most of the published IR spectra are the two bands in the middle of the spectrum. While the band around 1723 cm^{-1} was unambiguously assigned to a carbonyl group, the one at 1619 cm^{-1} has led to controversy. While some researchers attributed this band to the C═C bond, most researchers assigned it to water bending modes.[7,10,24] In separate experiments we confirmed assignment of the 1619 cm^{-1} absorption band to water molecules by acquiring FTIR spectra from deuterated GO samples (see Methods for details). Raising the pH of the solution increases the intensity of the 1619 cm^{-1} peak relative to the one at 1723 cm^{-1} (Figure 2b), suggesting higher water content in NaOH-GO compared to original GO. Note, the increase in the 1619 cm^{-1} peak intensity begins with a very small amounts of aqueous NaOH added to GO solution (pH < 5.0).

The TGA data (Figure 2c) of the original GO sample shows two major weight-loss regions: 17% in the 25−100 °C region, associated with the loss of physisorbed water, and 25.5% in the 150−200 °C region associated with decomposition of the functional groups. As is evident from Figure 2c, the thermal stability of solid NaOH-GO samples increases with the pH of solutions from which they are collected due to decrease in the oxygen functionality content. This is consistent with the XPS data (Figure 2a); the samples extracted from basic solutions are already significantly deoxygenated.

Absorbance in the visible-light region increases with the pH of the NaOH-GO solutions (Figure 2d) in accordance with visually observed darkening of solutions. In our previous work[17] we showed that darkening of as-prepared GO occurs even in pure water due to reaction with water. We can expect that in the basic solution this reaction will proceed to a greater extent. We have previously assigned the absorbance in the 200−250 nm region with the well-pronounced maximum at 230 nm to various oxygen functional groups. Absorbance in this region decreases with pH increase in accordance with XPS and TGA data (Figure 2a,c).

The ^{13}C SSNMR spectrum of the control GO sample (Figure 3) is qualitatively similar to those reported earlier.[7,9,18,19] The peaks at 61 and 70 ppm were previously assigned to epoxides and alcohols, respectively.[7,9,18,19]

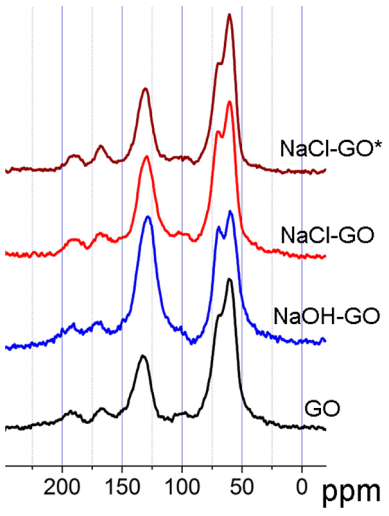

Figure 3. 50.3 MHz direct ^{13}C pulse MAS NMR spectra of the four GO samples. GO is collected from pure water solution; NaOH-GO is collected from the NaOH-added solution with pH = 10.13; NaCl-GO is collected from NaCl-added solution; and NaCl-GO* is collected from NaCl-added solution with prolonged exposure to NaCl: 12.0 kHz MAS; 60 s relaxation delay. Expanded plots of the centerband region are shown. The spectra are normalized with respect to the height of the signal at 61 ppm.

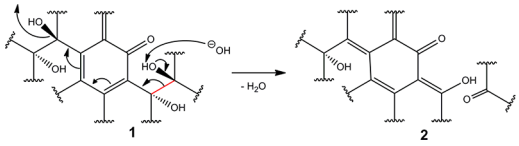

Scheme 1. Deoxygenation of GO under mild alkaline conditions. The structure 1 represents a GO fragment containing two vicinal diols and a ketone formed at a vacancy defect. Deoxygenation involves the C−C bond (red) cleavage, loss of two hydroxyl groups and formation of one ketone. Overall, 2 contains one less oxygen atom than 1.

The peak at 134 ppm is assigned to C═C carbon. Assignment of the weak downfield peaks, however, is not so straightforward. Because of their low intensities they have often been ignored. The peaks at 167 and 192 ppm, attributed to carbonyl-containing groups, originate from a relatively small number of carbon atoms. At the same time the role of these functional groups is important in understanding GO chemistry and structure.

The NaOH-GO sample recovered from the solution with pH of 10.13 (Figure 3) shows a profound difference in the spectrum when compared to the precursor GO sample. The intensities of the peaks at 61 and 70 ppm are significantly decreased relative to the intensity of the C═C peak at 134 ppm. These findings are consistent with the deoxygenation detected by XPS and TGA (Figure 2a,c). The NaCl-GO and NaCl-GO* spectra (Figure 3) will be discussed in the following sections.

Deoxygenation of GO in Alkaline Conditions. If the two conjugate bases titrated during the reverse titration (Figure 1b,c) are indeed carbonate and bicarbonate, then gaseous CO_2 might be produced. A series of

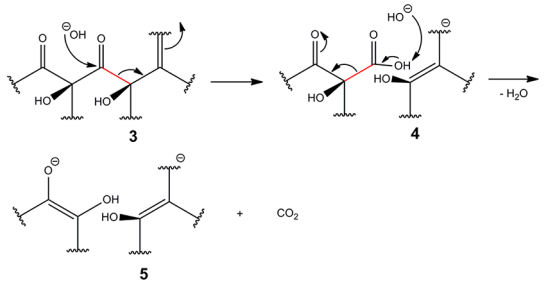

Scheme 2. Decarboxylation of GO under strong alkaline conditions. Structure 3 represents highly oxidized GO fragment. First, the nucleophilic attack of hydroxyl ion on the carbonyl results in C−C bond cleavage and formation of 4, containing a carboxyl group. Next, 4 decarboxylates to form 5 and carbon dioxide.

titration experiments was done while gases that were generated during the titration were collected. Indeed, a gas was generated during reverse titration, and the collected gas was identified as CO_2 by precipitation from a 1 M $Ba(OH)_2$ solution; IR analysis verified the precipitate as $BaCO_3$ (Supporting Information, Figure S2). To a great extent the amount of CO_2 collected varied from experiment to experiment. Normally little to no gas was collected during the forward titration, perhaps because the CO_2 reacted with OH− to yield HCO_3− and CO_3^{2-}. Some gas was collected in the course of the reverse titration, and a larger amount of gas was produced while the solution was standing after the reverse titration. On average, during the course of the forward−reverse titration and 48 h after the end of the reverse titration, the yield was one CO_2 molecule for every 21 carbon atoms from the original graphite lattice.

The XPS (Figure 2a) and ^{13}C SSNMR data (Figure 3) could lead to the conclusion that GO reduction is occurring, as was reported in ref 21 and 22, when GO was treated with a strong base. In terms of reduction−oxidation reactions, the observed phenomenon can instead be thought of as a disproportionation. The two stages of GO reaction with bases are as follows. First, under mild conditions, pH < 10.0 and room temperature, the epoxides and alcohols (formal oxidation state +1) disproportionate into elemental carbon with oxidation state 0 and a ketone with an oxidation state +2 as shown in eq 5 and Scheme 1. Note that **2** is a vinylogous carboxylic acid.

$$2C\text{—}OH \rightarrow \frac{1}{2}(C{=}C) + R_2C{=}O + H_2O \qquad (5)$$

Second, at pH > 10.0 and elevated temperatures, the reaction proceeds further, and CO_2 is produced as the highest oxidized form of carbon, as shown in eq 6 and Scheme 2. The summary reduction−oxidation eq 6 represents balancing of formal oxidation states of carbon atoms. Scheme 2 shows the corresponding transformation of a GO substructure.

$$4C\text{—}OH \rightarrow 1.5(C{=}C) + CO_2 + 2H_2O \qquad (6)$$

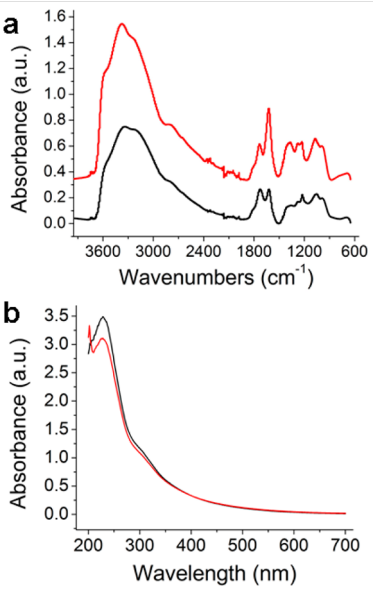

Figure 4. Spectral characteristics of the NaCl-GO samples. (a) FTIR spectra, (b) UV−vis absorbance spectra. The red line is the NaCl-GO; the black line is the control GO sample. The two spectra in panel a are normalized with respect to the 1723 cm^{-1} signal.

A rational way to form carbon dioxide is by a decarboxylation reaction; thus carboxyl groups should form first. It is logical to assume that carboxyl groups would form at the defects, terminated by ketones, where one out of three C−C bonds has been already cleaved. From the charge balance one can conclude that four hydroxyl-bonded carbon atoms can yield one CO_2 molecule (eq 6), thus making one carbon atom vacancy defect. Considering the high degree of alcohol functionality in GO, treating it with base produces the carbon material with a very high density of vacancy defects, making a single GO flake nonconductive. This may explain why no experimental electrical data were provided for the "base-reduced" GO samples.[20,21]

The Dynamic Structural Model. The NaOH solution which, as shown above, profoundly changes the GO chemical structure, contains two species capable of interaction with GO: Na^+ and OH−. The role of OH− is to facilitate the ionization of existing acidic groups and nucleophilic attack at active sites on GO as shown in Scheme 2. To investigate the role of Na^+, if any, we conducted a series of experiments where GO was exposed to an aqueous NaCl solution (see the Supporting Information for details). Thus Na^+ was introduced without changing the pH of the GO solution. The solid GO sample, recovered from the GO solution with NaCl addition will be referred to as NaCl-GO. The sample exposed to NaCl solution for a longer time, as compared to NaCl-GO, will be referred as NaCl-GO*; see Methods for more details.

The addition of NaCl did not cause GO solution darkening. Absorbance in the visible region was the same (Figure 4b) as for the precursor GO solution.

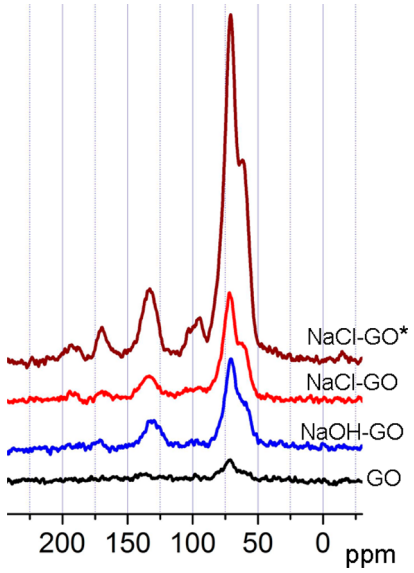

Figure 5. $^{1}H-^{13}C$ CPMAS NMR spectra for the four different GO samples: 7.6 kHz spinning; 1 ms contact time for cross-polarization; 33 ms FID; 5 s relaxation delay. The spectra are not normalized and were acquired with the following number of scans: GO, 33 000; NaOH-GO, 21 000; NaCl-GO, 16 800; NaCl-GO*, 16 400. Note that signal intensity increases in the order: GO, NaOH-GO, NaCl-GO, NaCl-GO*.

Absorbance in the UV region was noticeably decreased, as it was in the case of NaOH-GO (Figure 2d), suggesting the change in nature of oxygen functional groups. (The FTIR and UV–vis spectra of NaCl-GO and NaCl-GO* are almost identical, hence only NaCl-GO spectra are presented in Figure 4). The ^{13}C SSNMR data (Figure 3) did not show any profound difference between NaCl-GO and control GO samples, except a slightly higher content of carbonyls at 192 and 167 ppm (Supporting Information, Table S2).

Surprisingly, a profound difference between NaCl-GO and GO samples was found in their FTIR spectra. The spectrum of NaCl-GO sample was similar to the one for NaOH-GO: the 1619 cm^{-1} peak was larger relative to the 1723 cm^{-1} peak (Figure 4a). The intensity of the O–H stretch signal in the 3700–3200 cm^{-1} region also increased relative to the 1723 cm^{-1} signal, while the height of the shoulder at ~2700 cm^{-1} remained the same. These observations suggest higher water content in NaCl-GO compared to control GO.

Figure 5 shows the data for the cross-polarization, magic angle spinning (CPMAS) ^{13}C SSNMR experiment and can be compared to the direct pulse spectra in Figure 3. Under cross-polarization experimental conditions (Figure 5), carbon atoms will generate a signal only if they are located in close proximity to hydrogen atoms. The GO sample gives very low intensity signals with CPMAS ^{13}C SSNMR. The weak peak at ~70 ppm, corresponding to hydroxyl-bonded carbons, is the only distinguishable signal. The NaOH-GO and NaCl-GO samples generate more intense signals compared to GO. The NaCl-GO* sample generates a much stronger signal compared to the other three samples. Thus, the CPMAS ^{13}C SSNMR data suggest that there are more protons in close proximity to carbon atoms in the NaCl-GO and especially in the NaCl-GO* samples compared to the GO sample.

From CPMAS ^{13}C SSNMR (Figure 5) and FTIR (Figure 4) data one might conclude that GO samples exposed to sodium cations while in the solution phase stay more hydrated in the solid state. This is not exactly the case, however. Thus, according to TGA data (Supporting Information, Figure S3) there is a little difference in the water content: GO, NaCl-GO, and NaCl-GO* contain ~17%, ~18%, and ~20% of water, respectively, which is removed during the first wave of the weight loss (30–100 °C). XPS indicates that the three samples have almost the same C/O ratio which only slightly changes: 1.85, 1.83, and 1.79 for GO, NaCl-GO, and NaCl-GO*, respectively. Thus the difference between the samples is not in the quantity, but likely in the specific orientation of water molecules in NaCl-GO and NaCl-GO* toward the GO lattice, which results in stronger cross-polarization and in stronger FTIR absorbance.

Concerning the GO/water interface, it is known that in aqueous solution GO flakes are negatively charged.[12] This was confirmed by the zeta potentials (ζ) of *ca.* −50 mV obtained in this work. The electrical charge prevents flakes from coagulation and, along with the high surface area, facilitates stability of colloid solutions. The negatively charged GO flakes are surrounded by counterions, neutralizing the negative charge. According to the fundamentals of colloid chemistry,[28] the layer of counterions consists of two distinct parts: the inner layer, also known as the Helmholtz or Stern plane, and the diffuse layer, also known as the slipping plane. The inner monomolecular layer comprises ions and molecules strongly bonded to the GO surface *via* chemical interaction and can be considered as part of the GO flake. The ions in the diffuse layer are only loosely associated with the surface *via* Coloumbic interaction and actively exchange with ions from the bulk solution. This exchange reaction is a likely additional reason for the downward drifting pH observed during titration of the GO solutions with NaOH. It can also contribute to the lack of inflection points on the forward titration curves. When the concentration of H_3O^+ in the bulk solution is decreased by neutralization with added titrant, an active exchange reaction between the diffuse layer and the bulk solution begins: H_3O^+ from the diffuse layer migrates into the bulk solution, and Na^+ in turn replaces H_3O^+ in the diffuse layer.

To investigate the cation exchange reaction when NaCl but not NaOH is added to the GO solution, we conducted a series of experiments (see SI for details). As evident from Supporting Information, Table S1, the supernatant obtained by centrifugation of the GO solution is notably less acidic, compared to the original

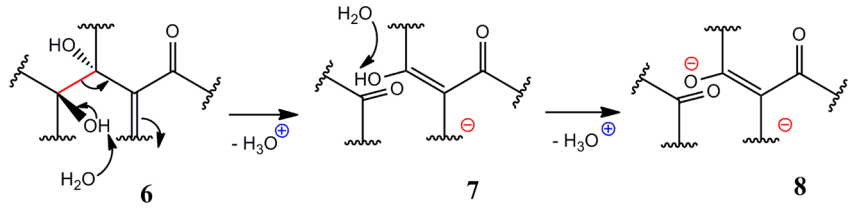

Scheme 3. Formation of a vinylogous carboxylic acid by ionization of a tertiary alcohol and C—C bond cleavage. In 6 the C—C bond to be cleaved is represented in red. Structure 7 contains a ketone and a vinylogous carboxylic acid formed as result of C—C bond cleavage. Structure 8 is an ionized form of 7, showing the vinylogous carboxylate.

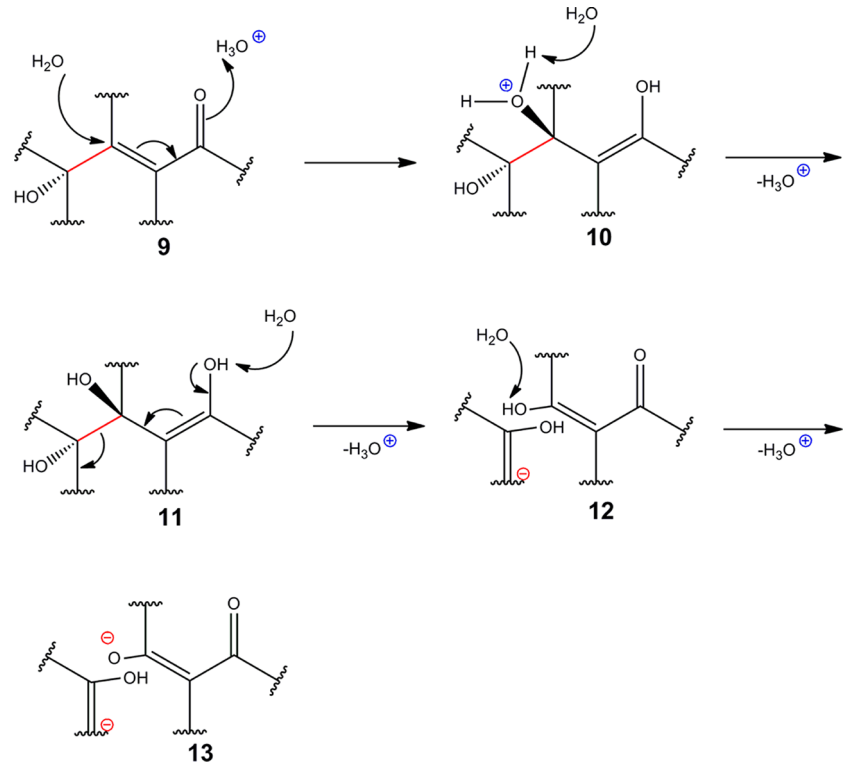

Scheme 4. Formation of vinylogous acid *via* attack of an extrinsic water molecule. Structure 9 is a GO fragment containing one hydroxyl group and one ketone. A water molecule enters the GO structure *via* conjugate (1,4) nucleophilic attack on 9, which yields intermediate 10 that is converted into enolic 11. Then 11, *via* C—C bond cleavage, is converted into the vinylogous acid 12. The vinylogous acid 12 ionizes to form anion 13.

solution. This observation suggests that GO flakes coprecipitate with H_3O^+. When NaCl is added to the GO solution, the acidity of the supernatant is almost the same as the acidity of the original NaCl-added GO solution. This suggests that Na^+ cations had successfully replaced the H_3O^+ ions.

Apparently, the Na^+ cations are more effective in building the counterion layer, which is demonstrated by the cation exchange reaction. Subsequently, introduction of Na^+ into a GO solution facilitates generation of higher negative charge on the GO layer compared to the charge in pure water. Thus ζ values were *ca.* −50 mV for the GO solution and *ca.* −56 mV for NaCl-GO solution (both at concentrations of 0.05 mg/mL). The addition of 0.025 M NaOH to the GO solution in the molar ratio C/NaOH = 2/1 increased ζ from −50 to −74 mV. These observations should not be viewed, however, as a simple conversion of carboxyl groups to carboxylate anions, as one might expect based on the LK model. The characteristic carboxylate peak at ~1580 cm^{-1} is not observable in the FTIR spectra of both NaCl-GO and NaOH-GO at pH < 10, and appears in the spectra of NaOH-GO samples collected from solutions with pH > 10 (Figure 2b, Figure 4a). Thus, strongly basic conditions are required to convert existing oxygen functionalities to carboxylates according to Scheme 2. The acid-to-salt conversion is in accord with the FTIR data, if one assumes that a vinylogous carboxylic acid, is converted to its respective salt, as in Schemes 3 and 4.

Thus, we consider the role of Na^+ ions simply as a feedstock for building an electrical double layer. By facilitating higher negative charge on GO flakes they accelerate the reaction between GO and water, which occurs even when no Na^+ ions are present, though at lower rates. We suggest that formation of the negative

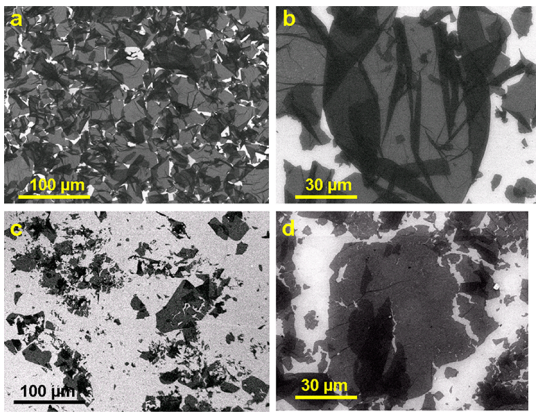

Figure 6. Degradation of GO in water. (a,b) SEM images of as prepared GO deposited on a Si/SiO_2 wafer. (c-d) SEM images of GO flakes that have been exposed to water for 2 months. The 0.5 mg/mL GO solution was kept 2 months without any agitation. The solution was swirled for 5 min before deposition on the wafer to disperse partially precipitated GO flakes. A gentle air stream was used to dry the wafers after dropcasting GO solution.

charge on GO flakes in aqueous solutions facilitates the observed transformations in the GO structure. Note that a water molecule from bulk solution needs to penetrate through the inner Helmholtz layer in order to react with GO. This lowers the rate of chemical reactions between GO and water.

Because of the complexity of the GO structure there are numerous possible scenarios for these reactions. Scheme 3 shows one of the possible reaction mechanisms where a negative electrical charge is built up on a GO platform.

Structure **6** shows the GO fragment containing a vicinal diol, formed by opening of epoxides, and a ketone, formed at the vacancy defect. The suggested reaction mechanism includes concerted ionization of one of the hydroxyl groups and the C−C bond cleavage. Scheme 3 represents the reaction in a neutral aqueous solution: the water molecule abstracts a proton. In basic solutions a hydroxide ion abstracts a proton far more readily and the reaction will progress faster. Note that the reaction produces hydrogen cation, thus acidifying the solution. The resulting **7** contains an enol conjugated with a carbonyl; together they make a vinylogous carboxylic acid. Ionization of the vinylogous acid lowers the pH of the solution. Structure **8**, the ionized form of **7**, is stabilized by resonance and by delocalization of a negative charge over the large sp^2-hybridized graphene domain in which the vinylogous acid is located. The accumulated negative charge in turn is neutralized by the layer of counterions as described above.

The proposed reaction mechanism (Scheme 3), suggesting formation of an additional carbonyl at the expense of a tertiary alcohol, is supported by the ^{13}C SSNMR data (Figure 3, Supporting Information, Table S2). The content of carbonyl carbons in NaCl-GO is higher compared to that in GO. The intensities of the 192 and 167 ppm signals increase at the expense of the 61 and the 70 ppm signals. Furthermore, the actual increase in carbonyl content might be higher than it appears based on the intensities of the 192 and 167 ppm signals. Earlier it was stated[17] that under the reaction conditions ketones are prone to be hydrolyzed with formation of gem-diols. The 101 ppm signal, earlier assigned to lactols,[19] can result from gem-diols. This signal is more intense in the spectrum of the NaCl-GO, compared to GO, which additionally supports its assignment to gem-diols. Thus, together with gem-diols (hydrolyzed ketones) the total increase in the content of carbonyls is ~8% for NaCl-GO compared to the GO sample (Supporting Information, Table S2).

The GO transformations shown in Schemes 1, 2, and 3 include C−C bond cleavage. Figure 6 shows further experimental evidence for such bond cleavage and demonstrates the GO flake destruction in water. Figure 6a,b shows GO flakes deposited on a Si/SiO_2 substrate from a freshly prepared GO solution. Figure 6c,d shows flakes deposited from a 2-month-old aqueous solution. GO flakes that have been exposed to water for a long time decompose into smaller pieces. Apparently, the GO flakes are one piece while in solution and break apart only when they come into contact with the surface of a Si/SiO_2 wafer due to the strain associated with deposition. Such breakage is possible only if a majority of the C−C bonds have been already cleaved by the time the GO flake comes into contact with the substrate surface. Thus, degradation of GO flakes during prolonged exposure to water is additional experimental evidence for the proposed reaction mechanism.

In the reaction mechanism shown in Scheme 3, the proton is produced from the hydroxyl moiety, which is an integral part of the GO structure. In Scheme 4 we propose an alternative reaction mechanism, where the proton is formed from the water molecule, which is originally extrinsic to the GO, but becomes a part of GO through chemical reaction. The sp^2-hybridized network of carbon atoms is resistant to any chemical attack, but the oxidized GO areas, containing sp^3-hybridized carbon atoms, are prone to chemical reaction.

The GO fragment **9** contains only one sp^3-hybridized carbon atom in close proximity to vacancy defects, terminated by a ketone. The water molecule conjugately attacks the carbon atom adjacent to the sp^3-hybridized atom and becomes a part of GO by forming an intermediate cation **10** that transforms to the structure **11**. This transformation yields one hydronium cation. The C−C bond cleavage in **11** yields the vinylogous acid **12**. This transformation is accompanied by an increase in the negative charge on the GO surface and with formation of an additional hydronium cation. Owing to formation of an electrical double

layer, the structure is prone to accumulate significant negative charge, facilitating ionization of vinylogous acid **12** into its ionized form **13**. Since the reaction involves nucleophilic attack by water and generation of H_3O^+ ions, the entire process might be slowed under acidic conditions.

To summarize our findings regarding the GO structure: we agree with the LK model that tertiary alcohols and epoxides are the main functional groups on the basal planes. Their presence is well supported by the observed GO chemistry and spectroscopic data. The carbonyls responsible for the 192 ppm ^{13}C SSNMR signal are likely the ketones conjugated with hydroxyls to form vinylogous carboxylic acids. The content of ordinary carboxyl groups, if any, does not exceed 3% based on the intensity of the 167 ppm ^{13}C SSNMR signal (Supporting Information, Table S2). Carboxyl groups can be considered as intermediate products leading to decarboxylation. Their content is self-regulated and maintained at a relatively low level.

Because of interaction with water, the structure of GO is constantly changing, which ends only with significant decomposition of the basal planes. The reaction of GO with water is accompanied by C−C bond cleavage and by generation of protons. Electrons released from the C−C bond cleavage are consumed in extension of the conjugation. Generation of hydrogen cations is accompanied by generation and accumulation of a negative charge on GO flakes that is stabilized by resonance and made more possible due to the high level of conjugation. The accumulated negative charge is neutralized by a positively charged layer of counterions near the surface of the flake. Concerning the C−C bond cleavage with formation of ketones, our DSM supports ideas proposed in the SD model. The spatial distribution of ketones, however, is different from the ribbon-like structure as proposed in the SD model. Ketones are formed randomly at vacancy defects and within the oxidized domains at the points of the C−C bond cleavage.

Interestingly, the pH downward drifting, similar to what we observed during titration of the GO samples, was previously observed during titration of humic acid.[29] The similarity suggests that the same chemistry is taking place during the titration, and the same type of functional groups are present both in GO and in humic acid. Humic acid is thought to be formed by decay of organic matter and known to be resistant to further decomposition. In the case of GO similar functional groups are produced, thus approaching the humic acid-like structures by oxidation of inorganic materials. Similarities in acidic properties of GO and humic acid suggest that this explanation of GO acidity, including the nature of the functional groups, could be extended to other types of carbon-based materials. If this is true, then conclusions about the nature and content of the oxygen surface groups in coke and coal, based on the Boehm titration protocols, are under question.

CONCLUSIONS

We propose a new GO model, which we call the DSM. In contrast with all the previously proposed models, we do not consider the GO as a static structure with a given set of functional groups. Instead, we suggest that new functional groups constantly develop and transform. The key role in all these transformations belongs to water, which incorporates into GO, transforming its structure, and then leaves the structure *via* different reactions. Our model explains the GO acidity not by dissociation of preexisting acidic groups (their content is very low), but by generation of hydrogen cations (protons) *via* constant reactions with water. The driving force of the transformations is accumulation of the negative charge on GO layers, which is stabilized by resonance and by formation of an electrical double layer. From the structural perspective, most of the carbonyls existing on the GO platform are associated with hydroxyls in the form of vinylogous acids; this renders the hydroxyl groups acidic. Prolonged exposure to water gradually degrades GO flakes, converting them into humic acid-like structures. In acidic conditions this process might be slower. For GO samples prepared by Staudenmaier's, Hummers', and improved Hummer's methods, hydrolysis of covalent sulfates contribute additionally to the integral acidity. We explain deoxygenation of GO in alkaline solutions by the disproportionation reaction resulting in formation of CO_2, vacancy defects and extension of conjugation. The traditionally used Boehm titration protocol conceals crucial information about the nature and content of oxygen functional groups in carbon-based materials.

METHODS

Preparing GO. *Oxidation of Graphite.* In a general procedure graphite flakes (Sigma-Aldrich, batch no. 13802EH; 6.00 g, 0.50 mol) were dispersed in 98% sulfuric acid (Fisher Scientific, L-13345; 800 mL) at room temperature using a mechanical stirrer. After 10 min of stirring, $KMnO_4$ (J. T. Baker, lot J41619; 6.00 g, 0.038 mol) was added. The mixture turned green due to the formation of the oxidizing agent MnO_3^+. Additional $KMnO_4$ (6.00 g, 0.038 mol) was added when the green color of MnO_3^+ was diminished, indicating that the oxidizing agent was consumed. It takes ~1 d to consume 1 $KMnO_4$ gram-equivalent. A total of 4 $KMnO_4$ portions were added one-by-one over 4 d. The end of the oxidation was determined by the disappearance of the green color after adding the fourth $KMnO_4$ equivalent. At the end of oxidation, the pink reaction mixture became very viscous due to exfoliation of the formed GO layers. The GO prepared by the described procedure was separated from the rest of the reaction mixture and purified as described in the following section.

Quenching and Washing of GO with Water. To obtain GO, the GO reaction mixture (180 g) was quenched in an ice−water mixture (500 mL). A 30% H_2O_2 solution (few drops) was added until the purple $KMnO_4$ color disappeared. Upon addition of the H_2O_2 the mixture turned light-yellow. After 20 min of swirling, the slurry was equally distributed among four 250 mL plastic centrifuge bottles and centrifuged at 4100 rpm (Sorval T1 centrifuge from Thermo Scientific) until the supernatant became clear and colorless, indicating complete conventional GO (cGO)[1] separation. It took ~2 h to separate the cGO from the rest of the reaction mixture after the first quench with the ice−water mixture. The precipitated cGO was redispersed in a new portion of water (500 mL), swirled for 1 h, and centrifuged again to separate cGO. In the following procedures for producing GO we refer to the sequence of these procedures (redispersing the precipitated GO in a new portion of water, followed by swirling, and then centrifugation to separate the GO) as 1 washing cycle. In all the experiments the centrifuge speed was 4100 rpm. The solutions were always centrifuged until the supernatant was clear and colorless. The centrifugation time required to reach complete separation was different and depended on the amount of remaining H_2SO_4 in the centrifuged mixture. When water was used as the solvent, it took from 4 to 24 h in different washing cycles to reach complete separation. After the first quench and separation, GO was water-washed 3× followed by 1 wash with 5% HCl and an additional water wash. The purified GO was dried under reduced pressure (~10 mmHg) at room temperature 2−3 d until the weight did not change. After drying, the GO sample was exposed to ambient conditions to equilibrate with atmospheric humidity.

Preparation of NaCl-GO, and NaCl-GO.* To prepare NaCl-GO, the fifth washing of GO was performed with 0.2 M NaCl instead of pure water; the 0.2 M NaCl solution was added to the GO precipitated after the fourth washing−centrifugation cycle in such an amount that the C/NaCl molar ratio was 2/1. The mixture was swirled for 30 min and centrifuged as described above. The resulted NaCl-GO was dried under reduced pressure (~10 mmHg) at room temperature 2−3 d until the weight did not change.

The NaCl-GO* was prepared as NaCl-GO with the only difference that the third, the fourth, and the fifth washings were performed with the 0.2 M NaCl solution.

Preparation of Deuterated GO Samples (D-GO). To prepare the D-GO, the regular GO sample was first dried above P_2O_5 at reduced pressure (P < 10 mmHg) in a desiccator for 7 d. Next, the P_2O_5 was removed and the D_2O was placed in a desiccator. The air was pumped out of the desiccator until P < 10 mmHg; the pumping was then stopped and the GO was hydrated with D_2O vapor for 24 h. The pumping−hydrating cycle was repeated three more times. The resulting D-GO was kept in the D_2O atmosphere until characterization.

Titration of GO Samples. For titration, 100 mg of solid GO was dispersed in 170 mL of distilled water by stirring under nitrogen until a fine brown colloid solution with no visible particulate matter was formed. It takes 2−10 h to fully dissolve solid GO in water. After GO was fully dissolved, the colloid solution was additionally equilibrated for 2 h under a stream of nitrogen with constant stirring. Forward titrations were performed with 0.100 M NaOH solutions from J. T. Baker and reverse titrations were performed with 0.100 M HCl from Fisher. Titrations were performed manually with a Fisher Science Education pH meter equipped with an Oakton combination electrode. The titrant was injected by 0.1 mL portions through the needle using the 1 mL-sized NORM-JECT syringe. The new portion of titrant was added when the pH was constant for ~15 s. All titrations and other pH measuring-related experiments were performed under a constant stream of nitrogen.

Characterization of GO samples. UV−vis absorbance spectra were obtained using a Shimadzu UV-3101PC UV−vis−NIR scanning spectrophotometer. FTIR spectra were recorded on a Nicolet ATR-FTIR spectrophotometer in the absorbance mode: 128 scans; resolutions 4 and 2. Direct ^{13}C pulse MAS NMR spectra were acquired on a Bruker Avance 200 spectrometer (50.3 MHz ^{13}C, 200.1 MHz ^{1}H) as previously described.[17] In particular, the spectra shown in Figure 3 were acquired with the 4 mm rotor spinning at 12.0 kHz (so that any spinning sidebands would be at ±238 ppm multiples from the centerband), 90° ^{13}C pulse, 41.0 ms FID acquisition time, 60 s relaxation delay for all samples. Relatively long relaxation delays were used to ensure meaningful relative signal intensities.[1] (For comparison, a spectrum of each sample was also obtained with just a 20 s relaxation delay.) The spectra obtained for each sample with 60 s delay and with 20 s delay were almost identical. Each FID was processed with 50 Hz (1 ppm) of line broadening. The number of scans used to obtain each spectrum: GO 4000, NaOH-GO 4000, NaCl-GO 5240, NaCl-GO* 4120. A cubic spline baseline correction (standard Bruker software) was applied to remove baseline curvature. For the cross-polarization, magic angle (CPMAS) ^{13}C SSNMR spectra: 7.6 kHz MAS spinning so that any spinning sidebands would be at ±151 ppm multiples from the centerband; 1 ms contact time; 33 ms FID; 5 s relaxation delay. The number of scans used to obtain each spectrum: GO, 33 000; NaOH-GO, 21 000; NaCl-GO, 16 800; NaCl-GO*, 16 400. Each FID was processed with 50 Hz (1 ppm) of line broadening. SEM images were acquired on a JEOL-6500 scanning electron microscope with 15 kV working voltage. TGA were acquired on a Q50 TGA from TA Instruments. The Z-potentials were measured using a Malvern Zen 3600 zetasizer based on the Smoluchowski equation.

Conflict of Interest: The authors declare no competing financial interest.

Acknowledgment. Funding for this project was provided by the Air Force Office of Scientific Research (FA9550-09-1-0581), Multi-Chem/Halliburton Group LLC, and MI SWACO/Schlumberger.

Supporting Information Available: Additional experimental data. This material is available free of charge *via* the Internet at http://pubs.acs.org.

REFERENCES AND NOTES

1. Dreyer, D. R.; Park, S.; Bielawski, W.; Ruoff, R. S. The Chemistry of Graphene Oxide. *Chem. Soc. Rev.* **2010**, *39*, 228–240.
2. Brodie, B. Note sur un Nouveau Procede pour la Purification et la Pesagregation du Graphite. *Ann. Chim. Phys.* **1855**, *45*, 351–353.
3. Hofman, U.; Holst, R. *Uber Saurenatur Methylierung Graphitoxyd* **1939**, *72*, 754–771.
4. Ruess, G. Uber das Graphytoxyhydroxyd (Graphitoxid). *Monatsh. Chem.* **1947**, *76*, 381–417.
5. Clauss, A.; Plass, R.; Boehm, H.-P.; Hofmann, U. Untersuchungen zur Structure des Graphitoxyds. *Z. Anorg. Allg. Chem.* **1957**, *291*, 205–220.
6. Scholz, W.; Boehm, H.-P. Betrachtungen zur Structur des Graphitoxids. *Z. Anorg. Allg. Chem.* **1969**, *369*, 327–340.
7. Mermoux, M.; Chabre, Y.; Rousseau, A. FTIR and ^{13}C NMR Study of Graphite Oxide. *Carbon* **1991**, *29*, 469–474.
8. Nakajima, T.; Mabuchi, A.; Hagiwara, R. A New Structure of Graphite Oxide. *Carbon* **1988**, *26*, 357–361.
9. Lerf, A.; He, H.; Forster, M.; Klinowski, J. Structure of Graphite Oxide Revisited. *J. Phys. Chem.* **1998**, *102*, 4477–4482.
10. Szabo, T.; Berkesi, Ot.; Forgo, P.; Josepovits, K.; Sanakis, Y.; Petridis, D.; Dekany, I. Evolution of Surface Functional Groups in a Series of Progressively Oxidized Graphite Oxide. *Chem. Mater.* **2006**, *18*, 2740–2749.
11. Stankovich, S.; Dikin, D. A.; Piner a, R. D.; Kohlhaas, K. A.; Kleinhammes, A.; Jia, Y.; Wu, Y.; Nguyen, S. T.; Ruoff, R. Synthesis of Graphene-Based Nanosheets *via* Chemical Reduction of Exfoliated Graphite Oxide. *Carbon* **2007**, *45*, 1558–1565.
12. Li, D.; Muller, M.; Gilje, S.; Kaner, R.; Wallace, G. Processable Aqueous Dispersions of Graphene Nanosheets. *Nat. Nanotechnol.* **2008**, *3*, 101–105.
13. Tang, V.; Allen, M.; Yang, Y.; Kaner, R. High-Throughput Solution Processing of Large Scale Graphene. *Nat. Nanotechnol.* **2009**, *4*, 25–29.

14. Erickson, K.; Erni, R.; Zonghoon Lee, Z.; Alem, N.; Will Gannett, A.; Zettl, A. Determination of the Local Chemical Structure of Graphene Oxide and Reduced Graphene Oxide. *Adv. Mater.* **2010**, *22*, 4467–4472.
15. Staudenmaier, L. Verfahren zur Darstellung der Graphitsäure. *Ber. Dtsch. Chem. Ges.* **1898**, *31*, 1481–1487.
16. Hummers, W. S.; Offeman, R. E. Preparation of Graphitic Oxide. *J. Am. Chem. Soc.* **1958**, *80*, 1339.
17. Dimiev, A.; Kosynkin, D. V.; Alemany, L. B.; Chaguine, P.; Tour, J. M. Pristine Graphite Oxide. *J. Am. Chem. Soc.* **2012**, *134*, 2815–2822.
18. Cai, W.; Piner, R. D.; Stadermann, F. J.; Park, S.; Shaibat, M. A.; Ishii, Y.; Yang, D.; Velamakanni, A.; An, S. J.; Stoller, M.; *et al*. Synthesis and Solid-State NMR Structural Characterization of ^{13}C-Labeled Graphite Oxide. *Science* **2008**, *321*, 1815–1817.
19. Gao, W.; Alemany, L. B.; Ci, L.; Ajayan, P. M. New Insights into the Structure and Reduction of Graphite Oxide. *Nat. Chem.* **2009**, *1*, 403–408.
20. Fan, X.; Peng, W.; Li, Y.; Li, X.; Wang, S.; Zhang, G.; Zhang, F. Deoxygenation of Exfoliated Graphite Oxide Under Alkaline Conditions: A Green Route to Graphene Preparation. *Adv. Mater.* **2008**, *20*, 4490–4493.
21. Wang, T.; Tian, H.; Wang, X.; Qiao, L.; Wang, S.; Wang, X.; Zheng, W.; Liu, Y. Electrical Conductivity of Alkaline-Reduced Graphene Oxide. *Chem. Res. Chin. Univ.* **2011**, *27*, 857–861.
22. Pei, S.; Cheng, H. The Reduction of Graphene Oxide. *Carbon* **2012**, *50*, 3210–3228.
23. Boehm, H. P.; Heck, W.; Sappok, R.; Diehl, E. Surface Oxides of Carbon. *Angew. Chem., Int. Ed.* **1964**, *3*, 669–677.
24. Szabo, T.; Tombacz, E.; Illes, E.; Dekany, I. Enhanced Acidity and pH-Dependent Surface Charge Characterization of Successively Oxidized Graphite Oxides. *Carbon* **2006**, *44*, 537–545.
25. Petit, C.; Seredych, M.; Bandosz, T. J. Revisiting the Chemistry of Graphite Oxides and Its Effect on Ammonia Adsorption. *J. Mater. Chem.* **2009**, *19*, 9176–9185.
26. Kovtyukhova, N. I.; Olliver, P. J.; Martin, B. R.; Mallouk, T. E.; Chizhik, S. A.; Buzaneva, E. V.; Gorchinskiy, A. D. Layer by Layer Assembly of Ultrathin Composite Films from Micron-Sized Graphite Oxide Sheets and Polycations. *Chem. Mater.* **1999**, *11*, 771–778.
27. Marcano, D. C.; Kosynkin, D. V.; Berlin, J. M.; Sinitskii, A.; Sun, Z.; Slesarev, A.; Alemany, L. B.; Lu, W.; Tour, J. M. Improved Synthesis of Graphene Oxide. *ACS Nano* **2010**, *4*, 4806–4814.
28. Hunter, R. J. *Introduction to Modern Colloid Science*; Oxford University Press: Oxford, New York, Melbourne, 1993.
29. Ritchie, J. D.; Perdue, E. M. Proton-Binding Study of Standard and Reference Fulvic Acids, Humic Acids, and Natural Organic Matter. *Geochim. Cosmochim. Acta* **2003**, *67*, 85–96.